

**Spectra Cathodoluminescence and Raman Imaging of Na-rich Feldspar and Maskelynite from The Villalbeto de la Peña Meteorite.** J. Garcia-Guinea<sup>1</sup>, L. Sanchez-Muñoz<sup>2</sup>, L. Tormo<sup>1</sup>, E. Crespo-Feo<sup>1</sup>, J. Ruiz<sup>3</sup>, A. I. Martin-Herrero<sup>4</sup>, A. Cremades<sup>3</sup>, <sup>1</sup>Museo Nacional Ciencias Naturales, Jose Gutierrez Abascal 2, Madrid 28006, Spain. <sup>2</sup>CIEMAT. Av. Complutense 22, Madrid 28040, Spain. <sup>3</sup>Centro de Biología Molecular, CSIC-Universidad Autónoma de Madrid, 28049 Cantoblanco, Madrid, Spain. <sup>4</sup>Seminario de Ciencias Planetarias, Universidad Complutense de Madrid, 28040 Madrid, Spain. <sup>5</sup>Dpto Física Materiales, Facultad de Fisicas, Universidad Complutense de Madrid, 28040 Madrid, Spain. Correspondence author: [l.tormo@mncn.csic.es](mailto:l.tormo@mncn.csic.es)

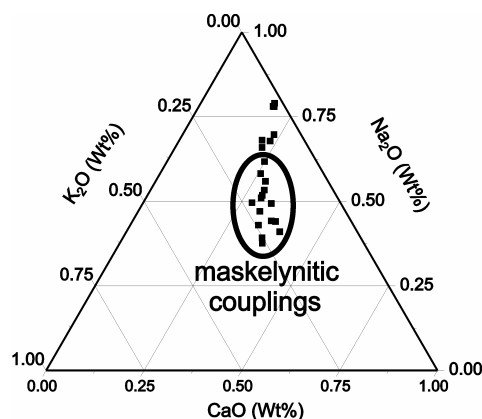
**Introduction:** The fall of the Villalbeto de la Peña meteorite on January 4, 2004 (Spain) is one of the best documented in history for which atmospheric and orbital trajectory, strewn field area, and recovery circumstances have been described in detail [1-2]. Additional details on the bulk chemistry [3] and the bulk luminescence [4] were later provided. Moreover, the intrinsic complexity of composition, distribution and structural states of plagioclase crystals in L6 chondritic meteorites [5], such as the Villalbeto feldspars case, suggested us to perform this study by Electron Probe Microanalyses (EPMA), spatially-resolved spectra Cathodoluminescence (CL) and Hyperspectral-Raman contour-plot micro-analyses (Raman), exploring the Maskelynite-Plagioclase distribution of the studied samples.

**Experimental:** We study polished sections of L6-chondrite specimens collected by ourselves in Villalbeto (Palencia). The Electron Probe Microanalyses (EPMA) were performed by a Jeol Superprobe JXA-8900M and by Environmental Scanning Electron Microscopy with X-ray Dispersive Spectrometry probe (ESEM-EDS) in a Inspect-S FEI company. Transmission electron microscopy (TEM micrographs and selected area electron diffraction (SAED) were obtained with a Tecnai20T (PHILIPS) microscope working at 200 kV. The hyperspectral Raman contour plots were performed using a new ThermoFischer Raman Microscope and a laser source at 532 nm. The hot cathodoluminescence (CL) spectra were obtained with an SEM-CL Hitachi S2500 electron microscope and a Hamamatsu PMA-11 CCD camera. Cold CL images of Villalbeto feldspars distribution were taken in a optical CL 8200 MK4 system of Cambridge Image Technology Ltd.

**Results and Discusión:** From the intensity of blue CL and BSE contrast in SEM images (Fig. 2a and b), two different regions of feldspatic composition have been observed: i) Maskelenite and Na-rich feldspars forming mixtures at a level lower than the resolution of optical microscopy techniques forming like-veins between other crystals and intergrowths with pyroxene; ii) extended volumes with homogeneous Na-rich feldspar crystalline structure. The results of the EPMA 45

spot analysis on feldspar phases are shown in both, Table 1, as some representative analyses of feldspar, and Figure 1, which displays the ternary Na<sub>2</sub>O—K<sub>2</sub>O—CaO compositions of Villalbeto feldspathic samples.

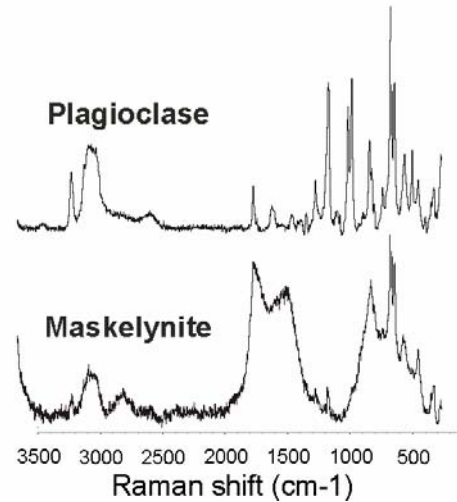
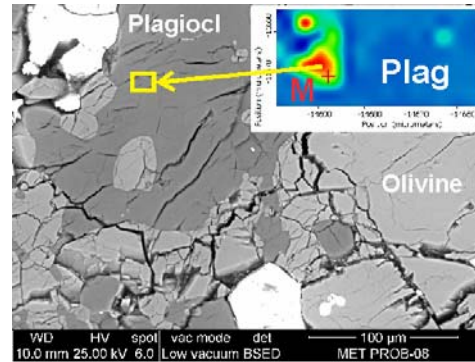
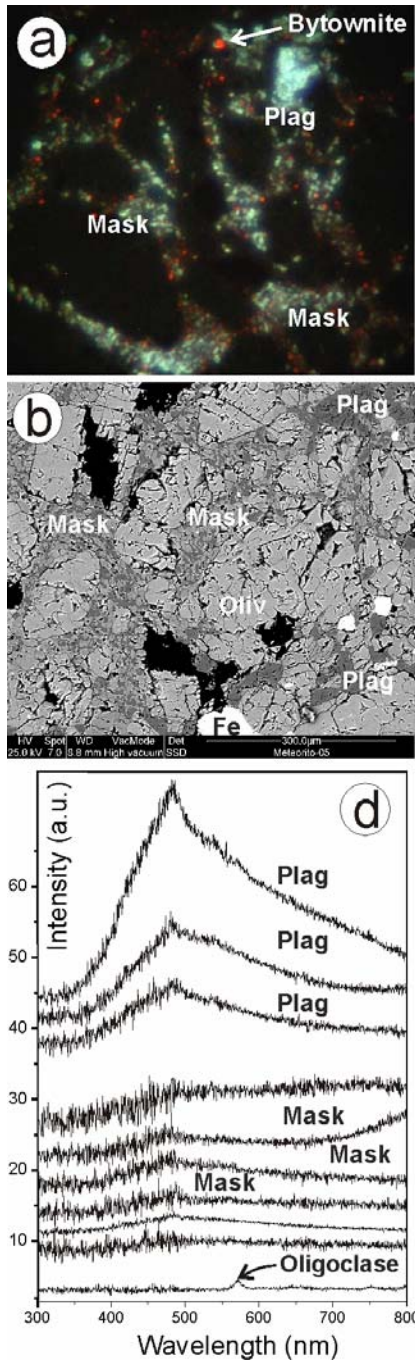
	Bytow.	Albit.	Oligo.	Mask.	Mask.
SiO <sub>2</sub>	64.63	64.87	66.15	67.84	68.81
Al <sub>2</sub> O <sub>3</sub>	17.58	21.18	22.87	23.28	22.96
FeO	1.41	0.44	0.54	0.31	0.66
MnO	0.01	0.00	0.08	0.00	0.00
MgO	3.76	0.01	0.02	0.00	0.03
CaO	8.20	2.36	2.51	2.24	2.16
Na <sub>2</sub> O	2.75	9.91	6.87	3.99	2.67
K <sub>2</sub> O	1.14	0.27	0.66	1.82	1.71
TiO <sub>2</sub>	0.10	0.00	0.02	0.01	0.09
NiO	0.03	0.01	0.00	0.00	0.10
Cr <sub>2</sub> O <sub>3</sub>	0.15	0.00	0.00	0.00	0.02
P <sub>2</sub> O <sub>5</sub>	0.03	0.02	0.03	0.00	0.00
Total	99.79	99.07	99.75	99.49	99.21



Na-rich feldspars were analyzed by transmission electron diffraction (TEM) and selected area electron diffraction (SAED) along [001] zone axis, in a microscope with an EDAX facility to correlate chemical, structural and microstructural data. No twinning were identified in TEM images, diffraction spots do not show splitting, and a regular circular shape allow us to measure the  $\gamma^*$  angle being lower than 90°, indicating a high or intermediate albite local ordering scheme in the Si/Al distribution. Maskelynite was easily identi-

fied by the lack of structure in the electron diffraction spectra. From our experimental results we infer that the metastable proportional K-Ca-Na compositions, sited in the triangle center, could be partially amorphous Maskelynite, together with plagioclase species, e.g., Bytownite, Albite, Oligoclase (Table 1).

tions, as follows: (i) red spots, Bytownite with  $Mn^{2+}$  point defects in structural Ca positions, (ii) blue masses, Oligoclase with  $[AlO_4]^\ominus$  defects, (iii) Maskelenite sodic glasses with low UV-blue emission. Figure 2b&c displays the spatially-resolved hot CL spectra taken on the feldspar masses observed by ESEM matching with the cold CL picture. A Hyper-spectral Raman plot was performed to explore the plagioclase crystal (Fig.3). The Maskeline amorphous phase was mainly observed in the Plagioclase fissures.



The Maskelenite Raman spectrum includes common peaks with plagioclases phases. This datum point to a tectonic origin for this, in accordance with previous data reported indicating that Villalbeto meteorite was not severely shok-metamorphosed [3]

**References:** [1] Llorca J. et al. (2005) *Meteoritics & Planet. Sci.*, 40, 795-804. [2] Trigo-Rodriguez J.M. et al. (2006) *Meteoritics & Planet. Sci.*, 41, 505-517. [3] Llorca J. et al. (2007) *Meteoritics & Planet. Sci.*, 41, A177-A182. [4] Correcher V. et al. (2007) *NIM Phys Res. A.* 580, 637-640. [5] Nakamura, Y. and Motomura, Y. (1999) *Meteoritics & Planet. Sci.*, 34, 763-772.

The meteorite luminescence is mainly produced by feldspars, Figure 2a shows its cold CL plot distribu-